REPORT DOCUMENTATION PAGE

AFRL-SR-AR-TR-02-

0181

The public reporting burden for this collection of information is estimated to average 1 hour per response, including th gathering and maintaining the data needed, and completing and reviewing the collection of information. Send comments of information, including suggestions for reducing the burden, to Department of Defense, Washington Headquarte. (0704-0188), 1215 Jefferson Davis Highway, Suite 1204, Arlington, VA 22202-4302. Respondents should be aware that notwithstanding any ~~~ ~~~ subject to any penalty for failing to comply with a collection of information if it does not display a currently valid OMB control number.
PLEASE DO NOT RETURN YOUR FORM TO THE ABOVE ADDRESS.

1. REPORT DATE *(DD-MM-YYYY)*	2. REPORT TYPE	3. DATES COVERED *(From - To)*
13-05-2002	Final Performance Report	15-12-2000 to 14-01-2002

4. TITLE AND SUBTITLE	5a. CONTRACT NUMBER
"Algorithm Development for the Two-Fluid Plasma Model"	F49620-01-1-0128

5b. GRANT NUMBER

5c. PROGRAM ELEMENT NUMBER

6. AUTHOR(S)	5d. PROJECT NUMBER
Uri Shumlak, Assistant Professor	

5e. TASK NUMBER

5f. WORK UNIT NUMBER

7. PERFORMING ORGANIZATION NAME(S) AND ADDRESS(ES)	8. PERFORMING ORGANIZATION REPORT NUMBER
Department of Aeronautics & Astronautics Box 352250, University of Washington Seattle, WA 98195-2250	

9. SPONSORING/MONITORING AGENCY NAME(S) AND ADDRESS(ES)	10. SPONSOR/MONITOR'S ACRONYM(S)
Air Force Office of Scientific Research 801 North Randolph Street, Room 732 Arlington, VA 22203-1977	AFSOR/PK

11. SPONSOR/MONITOR'S REPORT NUMBER(S)

20020614 165

13. SUPPLEMENTARY NOTES

14. ABSTRACT
A preliminary algorithm based on the two-fluid plasma model is developed to investigate the possiblity of simulating plasmas with a more physically accurate model than the MHD (magnetohydrodynamic) model. The algorithm is based on a Roe-type approximate Riemann solver. Beginning with the two-fluid plasma model, the governing equations are normalized and formulated in conservation form. The eigenvalues and eigenvectors of the system flux Jacobians are determined and properly normalized to prevent catastrophic cancellation. An approximate Reimann solver is developed based on the derived fluxes. The electromagnetic fields are solved and coupled to the two-fluid approximate Reimann solver. The field solver is an elctrostatic potential solver appropriate for electric fields and solves Poisson's equation.

15. SUBJECT TERMS

plasma, algorithm, Riemann solver, two-fluid plasma model, eigenvalues, eigendetectors

16. SECURITY CLASSIFICATION OF:			17. LIMITATION OF ABSTRACT	18. NUMBER OF PAGES	19a. NAME OF RESPONSIBLE PERSON
a. REPORT	b. ABSTRACT	c. THIS PAGE			Uri Shumlak
UU	UU	UU			**19b. TELEPHONE NUMBER** *(Include area code)* 206-616-1098 FAX 206-543-4719

Standard Form 298 (Rev. 8/98)
Prescribed by ANSI Std. Z39.18

ORIGINAL COPY

Algorithm Development for the Two-Fluid Plasma Model

U. Shumlak

Department of Aeronautics and Astronautics, Box 352250
University of Washington, Seattle, WA 98195-2250

Abstract

A preliminary algorithm based on the two-fluid plasma model is developed to investigate the possibility of simulating plasmas with a more physically accurate model than the MHD (magnetohydrodynamic) model. The algorithm is based on a Roe-type approximate Riemann solver. Beginning with the two-fluid plasma model, the governing equations are normalized and formulated in conservation form. The eigenvalues and eigenvectors of the system flux Jacobians are determined and properly normalized to prevent catastrophic cancellation. An approximate Riemann solver is developed based on the derived conserved fluxes. The electromagnetic fields are solved and coupled to the two-fluid approximate Riemann solver. The field solver is an electrostatic potential solver appropriate for electric fields and solves Poisson's equation. The algorithm is benchmarked against analytical results and published simulations. In a parallel effort, numerical methods for the calculation of the flux Jacobian were be investigated. The primary methods are the first-order limit formulation and the second-order complex number formulation.

Contents

List of Figures

1 Executive Summary

The primary objective of this project is perform the preliminary work to develop a plasma simulation algorithm based on the two-fluid plasma model. A two-fluid plasma simulation algorithm would be capable of time-dependent, three-dimensional simulations of plasma phenomena in realistic geometries. The algorithm would be a valuable tool for the design and testing of plasma related technologies that are important to the Air Force and industry, such as advanced plasma thrusters for space propulsion, hypersonic drag reduction, portable pulsed power, high power microwave devices, nuclear weapons effects simulations, radiation production for counter proliferation, and fusion for power generation. Implementing the algorithm on parallel supercomputers would allow the detailed modeling of realistic plasmas in complex three-dimensional geometries.

Current plasma simulation codes capable of complex geometries are based on the MHD (magnetohydrodynamic) model. The derivation of the MHD model involves several assumptions that severely limit its applicability. The two-fluid model only assumes local thermodynamic equilibrium. A two-fluid algorithm is more physically accurate and capable than MHD models. The two-fluid model is normalized and formulated in conservation form. The algorithm uses an approximate Riemann solver that we developed for the two-fluid plasma model. The algorithm is benchmarked against known analytical results and published simulations.

Several professional collaborations exist between the Department of Aeronautics and Astronautics at the University of Washington and the Air Force Research Laboratory both at Kirtland AFB and Edwards AFB, Los Alamos National Laboratory, Lawrence Livermore National Laboratory, the University of Michigan, Stanford University, and other departments at the University of Washington. The work from this project has been presented at international conferences.

2 Project Description

Plasmas are essential to many technologies that are important to the Air Force, some of which have dual-use potential. These applications include portable pulsed power systems, high power microwave devices, drag reduction for hypersonic vehicles, advanced plasma thrusters for space propulsion, nuclear weapons effects simulations, radiation production for counter proliferation, and fusion for power generation. In general, plasmas fall into a density regime where they exhibit both collective (fluid) behavior and individual (particle) behavior. The intermediate regime complicates the modeling of plasmas.

2.1 State of the Art — Kinetic, PIC, and MHD Models

Plasmas may be most accurately modeled using kinetic theory. The plasma is described by distribution functions in physical space, velocity space, and time, $f(\mathbf{x}, \mathbf{v}, t)$. The evolution of the plasma is then modeled by the Boltzmann equation.

$$\frac{\partial f_\alpha}{\partial t} + \mathbf{v}_\alpha \cdot \frac{\partial f_\alpha}{\partial \mathbf{x}} + \frac{q_\alpha}{m_\alpha}\left(\mathbf{E} + \mathbf{v}_\alpha \times \mathbf{B}\right) \cdot \frac{\partial f_\alpha}{\partial \mathbf{v}} = \left.\frac{\partial f_\alpha}{\partial t}\right|_{collisions} \tag{1}$$

1

for each plasma species α = ions, electrons. The Boltzmann equation coupled with Maxwell's equations for electromagnetic fields completely describe the plasma dynamics. [1–3]

However, the Boltzmann equation is seven dimensional. As a consequence of the large dimensionality plasma simulations using the Boltzmann equation are only used in very limited applications with narrow distributions, small spatial extent, and short time durations. [4,5] The seven dimensional space is further exacerbated by the high velocity space that is unused except for tail of the distribution or energetic beams. Boundary conditions are difficult to implement in kinetic simulations.

Particle in cell (PIC) plasma model apply the Boltzmann equation to representative superparticles which are far fewer (10^7) than the number of particles in the actual plasma (10^{20}). [6] PIC simulations have similar limitations as simulations using kinetic theory due to statistical errors caused by the fewer superparticles. Boundary conditions are also difficult to implement in PIC simulations.

The other end of the spectrum in plasma model involves taking moments of the Boltzmann equation and averaging over velocity space for each species which implicitly assumes local thermodynamic equilibrium. The resulting equations comprise the two-fluid plasma model. The two-fluid equations are then combined to form the MHD (magnetohydrodynamic) model. [7] However, in the process several approximations are made which limit the applicability of the MHD model to low frequency and ignores the electron mass and finite Larmor radius effects.

The MHD model treats the plasma like a conducting fluid and assigning macroscopic parameters to describe its particle-like interactions. Plasma simulation codes based on the MHD model have been very successful in modeling plasma dynamics and other phenomena. Codes such as MACH2 are based on arbitrary Lagrangian/Eulerian formulations. [8] ALE codes are well suited for simulating plasma phenomena involving moving interfaces. [9] However, ALE codes cannot be formulated as conservation laws and lack many of the inherent conservative properties.

We have successfully implemented the MHD model in conservative form to simulate realistic 3-D geometries. [10–12]

$$\frac{\partial Q}{\partial t} + \nabla \cdot \bar{\bar{T}}_h = \dot{Q}_{Non-ideal} \qquad (2)$$

where Q is the vector of conserved variables, $\bar{\bar{T}}_h$ is the tensor of hyperbolic fluxes, and $\dot{Q}_{Non-ideal}$ contains the non-ideal (mostly parabolic) terms. (For algorithm details we refer the reader to our published articles, Ph. D. dissertations, and previous AFOSR technical reports. [10–16]) We formulated the algorithm implicitly and demonstrated the superior accuracy and convergence over an explicit mode. Figure 1 shows the convergence history using the implicit algorithm. The algorithm uses a finite volume implementation with a block-structured domain that accommodates arbitrary shapes.

The lack of a divergence-free magnetic field is one of the most severe difficulties in algorithms which use the MHD model. The divergence of the magnetic field must be identically zero according to Maxwell's equation, $\nabla \cdot \mathbf{B} = 0$. A common remedy is to perform a Hodge projection to "clean" the divergence component of the field. We have added a divergence cleaner to our MHD algorithm. However, this adds a nonphysical step which still does not completely eliminate the divergence.

An even more severe limitation of the MHD model is the treatment the Hall effect and diamagnetic terms. These terms represent the separate motions of the ions and
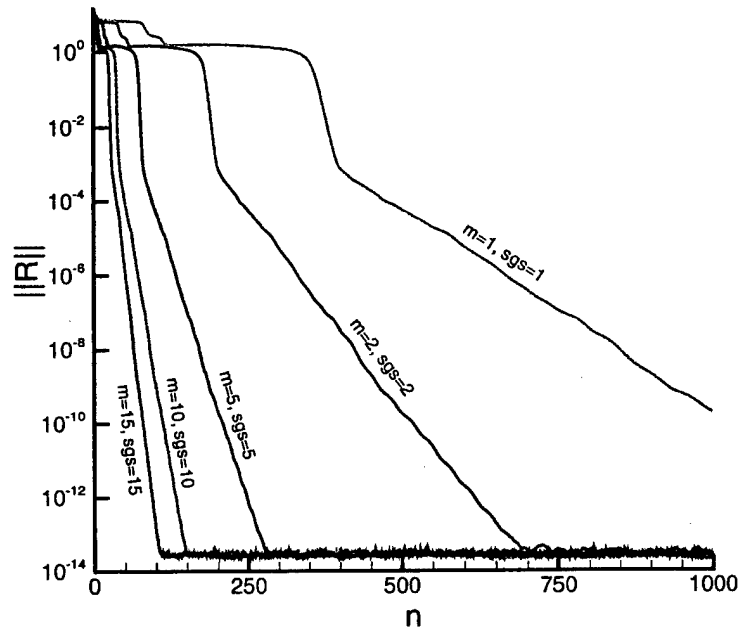
Figure 1: Convergence history using the SGS method to invert the implicit operator. n is the number of physical time iterations, m is the number of pseudo time subiterations, and sgs is the number of iterations of the SGS method.
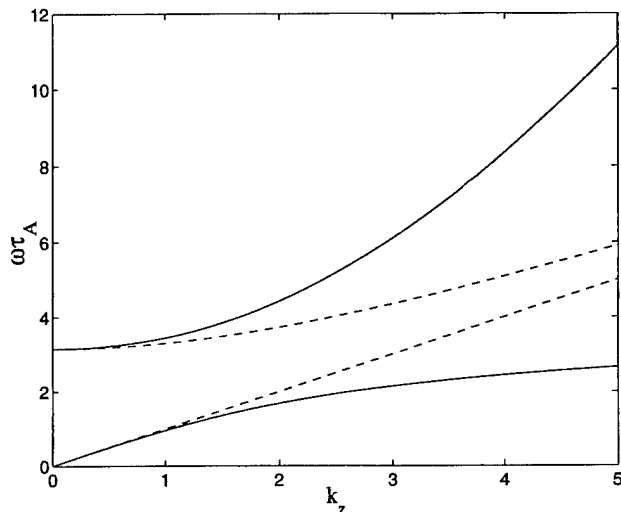
3

Figure 2: Dispersion relation for the fast and slow modes with $\omega_{ci}\tau_A = 3.5$. The dashed lines represent the ideal MHD modes.

electrons that still preserve the plasma approximation of quasineutrality. The Hall effect and diamagnetic terms also account for ion current and the finite Larmor radius of the plasma constituents. These effects are important in many applications such as electric space propulsion thrusters: Hall thrusters, magnetoplasmadynamic (MPD) thrusters, Lorentz force thrusters. The Hall term is also believed to be important to electrode effects such as anode and cathode fall which greatly affect many directly coupled plasma applications.

In general the Hall terms are difficult to stabilize because they lead to the whistler wave branch of the dispersion relation. The phase and group velocities of the whistler wave increase with frequency. See Figure 2 for the dispersion with a modest value of the Hall parameter $(\omega_{ci}\tau_A)^{-1}$.

We have treated the Hall term using a semi-implicit technique. [17, 18] After the hyperbolic terms of eqn(2) are advanced, the Hall terms are treated independently. The conserved variables are then corrected. The procedure can be computationally intensive. The operator stencil uses 5 points in the sweep direction and 3 points in the orthogonal direction. The complete operator stencil is 45 points. We have found that the semi-implicit method works adequately for small Hall parameters, but becomes unstable or slow to converge for large Hall parameters often seen in applications.

We have added multi-temperature capabilities to our MHD code. [16] The algorithm is based on an approximate Riemann solver to advance the conserved variables. The various energy loss and transfer mechanisms are then used to account for the change in temperature in each of the constituent species of the plasma and neutral gas. The multiple temperatures are then used to modify the ionization and recombination rate parameters. However, the (primary) hyperbolic algorithm is still a single fluid, single temperature.

4

2.2 The Next Step: Two-Fluid Plasma Model

The logical next step to extend the realistic geometry capabilities of the MHD model to the more physically accurate two-fluid model. The complexity of the two-fluid model is greater the MHD model but significantly less than the kinetic model.

The two-fluid model is derived by taking moments of the Boltzmann equation for each species. The process of taking moments eliminates the velocity space and yields a representative fluid velocity for each species. The model has the same dimensionality as the MHD model except there are two fluids. (The details of the model are described in Section 2.4.1.)

The physical accuracy of the two-fluid model is much better than the MHD model. The only approximation made is local thermodynamic equilibrium of each fluid but not with each other fluid.

The two-fluid plasma equations are normalized and formulated in conservative form. A high resolution approximate Riemann solver is derived that accurately calculates the transport of the conserved quantities. The algorithm is implemented using finite volumes to allow for extending the algorithm to three-dimensions and to model realistic general geometries with body fitted computational grids.

2.3 Research Objectives

The objectives of the proposed project are to:

- Derive an approximate Riemann solver for the two-fluid plasma model.

- Investigate possible methods for numerical evaluation of the flux Jacobian.

- Determine an appropriate flux limiter for the approximate Riemann solver to achieve a higher order accuracy algorithm.

- Formulate an electromagnetics algorithm and couple the algorithm to the approximate Riemann solver.

- Implement the algorithm with finite volume block-structured grids.

- Validate the code with analytical results.

2.4 Technical Description

This section describes the details of the two-fluid plasma model beginning from the two-fluid equations derived from moments of the Boltzmann equation. Further details about the derivation of the model can be found in most advanced plasma physics texts. See for example Ref. [19]. The proposed conservative formulation and algorithm are presented. The formulation has many properties which simplify the nature of the algorithm. These properties are discussed.

2.4.1 Two-Fluid Plasma Model

The two-fluid plasma model is derived by taking moments of the Boltzmann equation [eqn(1)] for each species. The process of taking moments averages over velocity space to yield a characteristic fluid velocity for the distribution of each species. The averaging

process implicitly assumes local thermodynamic equilibrium of each fluid. The moments are taken as:

$$\int \mathbf{X} \cdot \left(\frac{\partial f_\alpha}{\partial t} + \mathbf{v}_\alpha \cdot \frac{\partial f_\alpha}{\partial \mathbf{x}} + \frac{q_\alpha}{m_\alpha} \left(\mathbf{E} + \mathbf{v}_\alpha \times \mathbf{B} \right) \cdot \frac{\partial f_\alpha}{\partial \mathbf{v}} \right) d\mathbf{v} =$$

$$\int \mathbf{X} \cdot \left(\left. \frac{\partial f_\alpha}{\partial t} \right|_{collisions} \right) d\mathbf{v} \quad (3)$$

where $\mathbf{X} = 1, m_\alpha \mathbf{v}_\alpha, m_\alpha \left(\mathbf{v}_\alpha - \langle \mathbf{v} \rangle_\alpha \right)^2$ for each plasma species α = ions, electrons. The fundamental equations for the two-fluid model are generated by taking moments of the Boltzmann equation, and the fundamental variables are generated by taking moments of the distribution function.

Maxwell's equations describe the evolution of the electromagnetic fields. The fields couple to the ion and electron fluid variables and complete the model.

$$\nabla \cdot \mathbf{E} = e(n_i - n_e)/\epsilon_o$$
$$\nabla \cdot \mathbf{B} = 0$$
$$\frac{\partial \mathbf{B}}{\partial t} = -\nabla \times \mathbf{E} \quad (4)$$
$$\epsilon_o \frac{\partial \mathbf{E}}{\partial t} = \nabla \times \mathbf{B}/\mu_o - \mathbf{j}$$

The evolution of the particle density of the ions and electrons is expressed by continuity equations with the source term equal to the difference of electron and ion ionizations and recombination. This is also the zeroth moment of the Boltzmann equation.

$$\frac{\partial n_i}{\partial t} + \nabla \cdot (n_i \mathbf{v}_i) = S_{i,e} \quad (5)$$
$$= n_n n_i \langle \sigma v \rangle_{i-ion} + n_n n_e \langle \sigma v \rangle_{e-ion} - n_i n_e \langle \sigma v \rangle_{recomb}$$

$$\frac{\partial n_e}{\partial t} + \nabla \cdot (n_e \mathbf{v}_e) = S_{i,e} \quad (6)$$

where n_i, n_e, n_n are the ion, electron, neutral number densities, $\mathbf{v}_i$, $\mathbf{v}_e$, are the ion and electron fluid velocities, and $\langle \sigma v \rangle$ are the interaction rate parameters for ion and electron impact ionization and recombination. Partial current densities can be defined as

$$\mathbf{j}_i = e n_i \mathbf{v}_i, \text{ and } \mathbf{j}_e = e n_e \mathbf{v}_e. \quad (7)$$

where e is the electronic charge. The derivation presented here assumes singly ionized species, $q = e$. (For multiple charged ions, $n_e \to Z n_e$ where Z is the charge state.) Using the partial current densities, the particle continuity equations are then written as

$$\frac{\partial n_i}{\partial t} + \frac{1}{e} \nabla \cdot \mathbf{j}_i = S_{i,e}, \quad (8)$$

and

$$\frac{\partial n_e}{\partial t} - \frac{1}{e} \nabla \cdot \mathbf{j}_e = S_{i,e} \quad (9)$$

6

The first moment of the Boltzmann equation yields momentum equations for each species.

$$n_i m_i \left[\frac{\partial \mathbf{v}_i}{\partial t} + (\mathbf{v}_i \cdot \nabla) \mathbf{v}_i \right] =$$
$$- \nabla p_i + n_i e \left(\mathbf{E} + \mathbf{v}_i \times \mathbf{B} \right) + \mathbf{R}_{ei} - n_i m_i \mathbf{v}_i \nu_{in} \quad (10)$$

$$n_e m_e \left[\frac{\partial \mathbf{v}_e}{\partial t} + (\mathbf{v}_e \cdot \nabla) \mathbf{v}_e \right] =$$
$$- \nabla p_e - n_e e \left(\mathbf{E} + \mathbf{v}_e \times \mathbf{B} \right) - \mathbf{R}_{ei} - n_e m_e \mathbf{v}_e \nu_{en} \quad (11)$$

where $\mathbf{E}$ and $\mathbf{B}$ are the electric and magnetic fields, p_i and p_e are the ion and electron partial pressures, $\mathbf{R}_{ei}$ is the electron to ion momentum transfer vector, and ν_{in} and ν_{en} are the ion-neutral and electron-neutral collision frequencies.

Substituting the definitions of partial current densities and using eqns(8) and (9), the momentum equations are rewritten in conservative form for the partial current densities.

$$\frac{\partial \mathbf{j}_i}{\partial t} + \nabla \cdot \left(\frac{\mathbf{j}_i \mathbf{j}_i}{e n_i} + \frac{e}{m_i} p_i \bar{\bar{I}} \right) =$$
$$\frac{e^2 n_i}{m_i} \mathbf{E} + \frac{e}{m_i} \mathbf{j}_i \times \mathbf{B} + \frac{e}{m_i} \mathbf{R}_{ei} - \mathbf{j}_i \left(\nu_{in} - \frac{S_{i,e}}{n_i} \right) \quad (12)$$

$$\frac{\partial \mathbf{j}_e}{\partial t} - \nabla \cdot \left(\frac{\mathbf{j}_e \mathbf{j}_e}{e n_e} + \frac{e}{m_e} p_e \bar{\bar{I}} \right) =$$
$$\frac{e^2 n_e}{m_e} \mathbf{E} - \frac{e}{m_e} \mathbf{j}_e \times \mathbf{B} + \frac{e}{m_e} \mathbf{R}_{ei} + \mathbf{j}_e \left(\nu_{en} + \frac{S_{i,e}}{n_e} \right) \quad (13)$$

The second moment of the Boltzmann equation yields energy equations for each species.

$$\frac{3}{2} n_i \left[\frac{\partial T_i}{\partial t} + (\mathbf{v}_i \cdot \nabla) T_i \right] = -p_i \nabla \cdot \mathbf{v}_i - \nabla \cdot \mathbf{q}_i + P_{ext_i} - P_{cx} \quad (14)$$

$$\frac{3}{2} n_e \left[\frac{\partial T_e}{\partial t} + (\mathbf{v}_e \cdot \nabla) T_e \right] = -p_e \nabla \cdot \mathbf{v}_e - \nabla \cdot \mathbf{q}_e + P_{ext_e} - P_{rad} \quad (15)$$

where T_i, T_e are the ion and electron temperatures, $\mathbf{q}_i$, $\mathbf{q}_e$ are the ion and electron heat fluxes, P_{ext_i}, P_{ext_e} are external input powers, P_{cx} is the charge exchange power, and P_{rad} is the radiated power. The temperatures are related to the partial pressures by

$$p_\alpha = n_\alpha T_\alpha \quad (16)$$

for $\alpha = \{i, e\}$. The energy equations can be combined with the corresponding momentum equations to yield energy equations expressed in conservative form for the total energy.

$$\frac{\partial \varepsilon_i}{\partial t} + \nabla \cdot \left[(\varepsilon_i + p_i) \frac{\mathbf{j}_i}{e n_i} \right] = \mathbf{j}_i \cdot \left(\mathbf{E} + \frac{\mathbf{R}_{ei}}{e n_i} \right) - \frac{m_i j_i^2}{e^2 n_i} \nu_{in} + \frac{\varepsilon_i S_{i,e}}{n_i} \quad (17)$$

$$\frac{\partial \varepsilon_e}{\partial t} - \nabla \cdot \left[(\varepsilon_e + p_e) \frac{\mathbf{j}_e}{e n_e} \right] = \mathbf{j}_e \cdot \left(\mathbf{E} + \frac{\mathbf{R}_{ei}}{e n_e} \right) - \frac{m_e j_e^2}{e^2 n_e} \nu_{en} + \frac{\varepsilon_e S_{i,e}}{n_e} \tag{18}$$

where the total energy is defined by

$$\varepsilon_i \equiv \frac{3}{2} n_i T_i + \frac{1}{2} n_i m_i v_i^2 = \frac{3}{2} p_i + \frac{1}{2} n_i m_i v_i^2 \tag{19}$$

and

$$\varepsilon_e = \frac{3}{2} p_e + \frac{1}{2} n_e m_e v_e^2. \tag{20}$$

2.4.2 Conservative Algorithm

The two-fluid plasma model is now expressed in conservative form.

$$\frac{\partial Q}{\partial t} + \nabla \cdot \bar{\bar{T}}_h = \dot{Q}_{force} \tag{21}$$

where Q is the vector of conserved variables, $\bar{\bar{T}}_h$ is the tensor of hyperbolic fluxes, and $\dot{Q}_{force}$ is the forcing function. The vector of conserved variables is

$$Q = \begin{bmatrix} n_i \\ n_e \\ j_{i_x} \\ j_{i_y} \\ j_{i_z} \\ j_{e_x} \\ j_{e_y} \\ j_{e_z} \\ \varepsilon_i \\ \varepsilon_e \end{bmatrix}. \tag{22}$$

The hyperbolic flux tensor in the x direction is

$$F = \begin{bmatrix} \frac{j_{i_x}}{e} \\ -\frac{j_{e_x}}{e} \\ \frac{j_{i_x}^2}{e n_i} + \frac{e}{m_i} p_i \\ \frac{j_{i_x} j_{i_y}}{e n_i} \\ \frac{j_{i_x} j_{i_z}}{e n_i} \\ -\frac{j_{e_x}^2}{e n_e} - \frac{e}{m_e} p_e \\ -\frac{j_{e_x} j_{e_y}}{e n_e} \\ -\frac{j_{e_x} j_{e_z}}{e n_e} \\ (\varepsilon_i + p_i) \frac{j_{i_x}}{e n_i} \\ -(\varepsilon_e + p_e) \frac{j_{e_x}}{e n_e} \end{bmatrix}. \tag{23}$$

The characteristic velocities will then be calculated to construct the approximate Riemann fluxes.

In 1-D with an assumed ratio of specific heats $\gamma = 5/3$, the flux Jacobian for the two-fluid equations is

$$
\frac{\partial F}{\partial Q} = \begin{bmatrix}
0 & 0 & \frac{1}{e} \\
0 & 0 & 0 \\
-\frac{2}{3}\frac{j_{i_x}^2}{en_i^2} & 0 & \frac{4}{3}\frac{j_{i_x}}{en_i} \\
0 & \frac{2}{3}\frac{j_{e_x}^2}{en_e^2} & 0 \\
-\frac{j_{i_x}}{en_i}\left(\frac{5}{2}\frac{p_i}{n_i} + \frac{1}{6}\frac{m_i j_{i_x}^2}{e^2 n_i^2}\right) & 0 & \frac{5}{2}\frac{p_i}{en_i} - \frac{1}{6}\frac{m_i j_{i_x}^2}{e^3 n_i^2} \\
0 & \frac{j_{e_x}}{en_e}\left(\frac{5}{2}\frac{p_e}{n_e} + \frac{1}{6}\frac{m_e j_{e_x}^2}{e^2 n_e^2}\right) & 0
\end{bmatrix}
$$

$$
\begin{bmatrix}
0 & 0 & 0 \\
-\frac{1}{e} & 0 & 0 \\
0 & \frac{2}{3}\frac{e}{m_i} & 0 \\
-\frac{4}{3}\frac{j_{e_x}}{en_e} & 0 & -\frac{2}{3}\frac{e}{m_e} \\
0 & \frac{5}{3}\frac{j_{i_x}}{en_i} & 0 \\
-\frac{5}{2}\frac{p_e}{en_e} + \frac{1}{6}\frac{m_e j_{e_x}^2}{e^3 n_e^2} & 0 & \frac{5}{3}\frac{j_{e_x}}{en_e}
\end{bmatrix} \quad (24)
$$

The eigenvalues of the flux Jacobian give the characteristic velocities.

$$
\lambda = \left\{ \frac{j_{i_x}}{en_i}, \frac{j_{i_x}}{en_i} \pm \sqrt{\frac{5}{3}\frac{T_i}{m_i}}, -\frac{j_{e_x}}{en_e}, -\frac{j_{e_x}}{en_e} \pm \sqrt{\frac{5}{3}\frac{T_e}{m_e}} \right\} \quad (25)
$$

Acoustic speeds are defined as

$$
\begin{aligned}
c_{s_i}^2 &= \frac{5}{3}\frac{T_i}{m_i} = \frac{5}{3}\frac{p_i}{m_i n_i} \\
c_{s_e}^2 &= \frac{5}{3}\frac{T_e}{m_e} = \frac{5}{3}\frac{p_e}{m_e n_e}
\end{aligned} \quad (26)
$$

The presence of a complete set of eigenvalues proves that the system is hyperbolic. An approximate Riemann solver is appropriate. The eigenvalues for the two-fluid plasma model represent the combination of the drift speeds and thermal speeds for the electrons and ions. The speeds for the electrons are expected to be quite large, but much less than the speed of light. The large span of the eigenvalues makes the system stiff and more difficult to solve, particularly with an implicit method. The stiffness of the equations, particularly the source terms, is solved by treating the source terms implicitly. The details are described in Sec. 3.1.3.

The hyperbolic fluxes of eqn(21) are discretized using a Roe-type approximate Riemann solver. [20] In this method the overall solution is built upon the solutions to the Riemann problem defined by the discontinuous jump in the solution between each pair of cells. The numerical flux for a first-order accurate (in space) Roe-type solver is written in symmetric form as

$$
F_{i+1/2} = \frac{1}{2}\left(F_{i+1} + F_i\right) - \frac{1}{2}\sum_k l_k \left(Q_{i+1} - Q_i\right)|\lambda_k| r_k \quad (27)
$$

where r_k is the kth right eigenvector, λ_k is the absolute value of the kth eigenvalue, and l_k is the kth left eigenvector. The values at the cell interface $(i + 1/2)$ are obtained
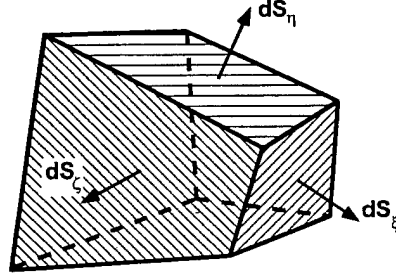
Figure 3: Schematic of the arbitrary shaped three-dimensional finite volume cell to be used by the two-fluid algorithm.

either by a simple average or by forming a more accurate Roe-average of the neighboring cells. The flux calculated as above is normal to the cell interface which is the desired orientation for applying the divergence theorem in a finite volume method. A typical three-dimensional, finite-volume grid cell is shown in Figure 3.

The solution of Maxwell's equations [eqn(4)] is required at each time. For the preliminary, one-dimensional algorithm developed in this stage of the project, a magnetostatic model for the electromagnetic fields is assumed. The electric field is determined by solving Poisson's equation with the charge density and the introduction of the electrostatic potential, ϕ. Maxwell's equations then become

$$\nabla \cdot \mathbf{E} = -\nabla^2 \phi = e(n_i - n_e)/\epsilon_o. \tag{28}$$

The applied magnetic field is constant. An assumption of quasineutrality $(n_i = n_e)$ is not necessary.

3 Project Implementation and Results

3.1 Algorithm Details

The two-fluid algorithm has been successfully implemented in one-dimension with an electrostatic field model. Ampere's law was modified by including an electrostatic potential which improves the quality of the solution for larger λ_D ($\lambda_D \approx L$) simulations by generating electric fields that simultaneously satisfy Ampere's law and Poisson's equation. The stiffness of the two-fluid equations was relaxed by implicitly treating the non-homogeneous source terms. The homogeneous fluxes were calculated using an approximate Riemann solver for each fluid. The non-homogeneous sources terms were then solved implicitly to complete the two-fluid solutions.

3.1.1 Maxwell's Equations with Electrostatic Potential Correction

Maxwell's equations couple the electron fluid with the ion fluid through the non-dimensional field equations. Ampere's law describes the time evolution of the electric

10

field in the presence of currents and magnetic fields.

$$\epsilon_o \frac{\partial \mathbf{E}}{\partial t} = \nabla \times \mathbf{B}/\mu_o - \mathbf{j} \tag{29}$$

However, the discretized equations do not guarantee the calcualted electric field satisfies Poisson's equation [eqn(28)] which describes the electrostatic electric field generated by a collection of charges. This problem is similar to the numerical generation of magnetic fields that are not divergence-free. Using the technique of Munz [21], Maxwell's equations were re-written to include an electrostatic potential, ϕ, which propagated the error in eqn(28) out of the domain at the speed Γ. The modified equations became

$$\epsilon_o \mu_o \frac{\partial \mathbf{E}}{\partial t} = \nabla \times \mathbf{B} + \nabla \phi - \mathbf{j} \tag{30}$$

and

$$\frac{\partial \phi}{\partial t} - \Gamma^2 \nabla \cdot \mathbf{E} = \Gamma^2 e(n_i - n_e)/\epsilon_o. \tag{31}$$

3.1.2 Homogeneous Fluxes

The two fluid system just described consists of two hyperbolic systems, electron fluid and ion fluid, which are coupled through Maxwell's equations source terms. It is important to note that the homogeneous part of the electron system depends only on the electron fluid variables, and the homogeneous part of the ion system depends only on the ion variables. As a result, separate Riemann solvers are used to solve the homogeneous parts of the electron fluid and the ion fluid. Each of the homogeneous hyperbolic systems is written in the form

$$\frac{\partial Q}{\partial t} + \nabla \cdot \bar{\bar{T}}_h = 0 \tag{32}$$

where Q is the vector of piece-wise-constant, conserved variables and $\bar{\bar{T}}_h$ is the tensor of hyperbolic fluxes, as defined in eqns(22) and (23).

The approximate Riemann solver solves the one-dimensional Riemann problems across each cell interface. Consequently, it is only necessary to include the flux perpendicular to a face in our discretization. The discretized homogeneous hyperbolic equations are solved as presented in Sec. 2.4.2.

The modified Maxwell's equations are solved with an approximate Riemann solver where the conserved vector is

$$Q = \begin{bmatrix} B_x \\ E_x \\ \phi \end{bmatrix} \tag{33}$$

and the flux vector is

$$F = \begin{bmatrix} 0 \\ \phi \\ \Gamma^2 E_x \end{bmatrix} \tag{34}$$

For each system a matrix A is calculated such that $\Delta F = A \Delta Q$. For Maxwell's equations, A is simply the flux Jacobian matrix $\frac{\partial F}{\partial Q}$. For the fluid systems, A is the Roe matrix based on the flux Jacobian. [22] The eigenvalues, eigenvectors and characteristic waves are calculated from the A matrix.

11

3.1.3 Implicit Treatment of the Source Terms

The stiffness of the two-fluid algorithm was generated by the large value of the right hand side of eqn(21). Therefore, the source terms are updated implicitly at which point the three separate systems (electron fluid, ion fluid, and electromagnetic fields) are treated as one large system. The full discretized equation with implicit source terms is

$$\frac{Q^{n+1} - Q^n}{\Delta t} = \frac{A}{V} \left(F^n_{i+1/2} - F^n_{i-1/2} \right) + \psi^{n+1} \tag{35}$$

where ψ^{n+1} is the source term evaluated at the $n+1$ time step. The source term is expanded in a Taylor series to first order and the resulting Newton iteration is written as

$$\left(\frac{1}{\Delta t} - \frac{\partial \psi^k}{\partial Q^k} \right) \Delta Q = -\frac{Q^k - Q^n}{\Delta t} - \frac{A}{V} \left(F^n_{i+1/2} - F^n_{i-1/2} \right) + \psi^k \tag{36}$$

where $\Delta Q = Q^{n+1} - Q^k$ and k is the iteration variable.

After the numerical fluxes are calculated explicitly as described in the previous section, the source terms are solved implicitly. Within each iteration the linear system, eqn(36), is solved using a symmetric Gauss-Seidel method. The flux Jacobian in eqn(36) is recalculated and Q is updated after each iteration until the 2-norm of ΔQ has dropped by several orders of magnitude. after approximately three iterations. It is important to note that $\frac{\partial \psi^k}{\partial Q^k}$ is local, and ψ does not depend on the value of Q in adjacent cells. This means that the computational work required to solve eqn(36) increases linearly with the number of cells in our domain, even when the algorithm is extended to three dimensions.

In many cases the different solvers can be updated using different time steps. For example, for MHD like problems the ion equations can be ignored for several time steps so a simplified system consisting only of Maxwell's equations and the electron equations is used. After several time steps the full system is used and the ion fluid is updated. The choice of time step depends on the respective stiffness of the source terms for each solver as well as the hyperbolic wave speeds.

3.2 Coplanar Riemann Problem

The preliminary algorithm was tested for its ability to capture shock and its ability to capture plasma phenomena such as Langmuir oscillations.

The coplanar Riemann (or shock tube) problem is used to test the fundamental behavior of the approximate Riemann solver. As expected from an approximate Riemann solver, wave structures are well captured. The behavior is best seen when the effect of the electromagnetic fields is eliminated by artifically setting the electron and ion charge to zero and reducing the effect of the large mass difference by setting the electron mass to 20% of the ion mass, $m_e = 0.2m_i$. The electron and ion fluids then decouple and behave as independent fluids. Results are shown in Figs. 4 and 5. The coplanar Riemann problem is initiated with normalized electron and ion number densities of 4.0 on the right hand side of the domain and 1.0 on the left hand side of the domain. The normalized electron and ion temperatures are initialized at a uniform value of 10. The domain is discretized into 256 volumes. Fig. 4 shows the evolution of the electron and
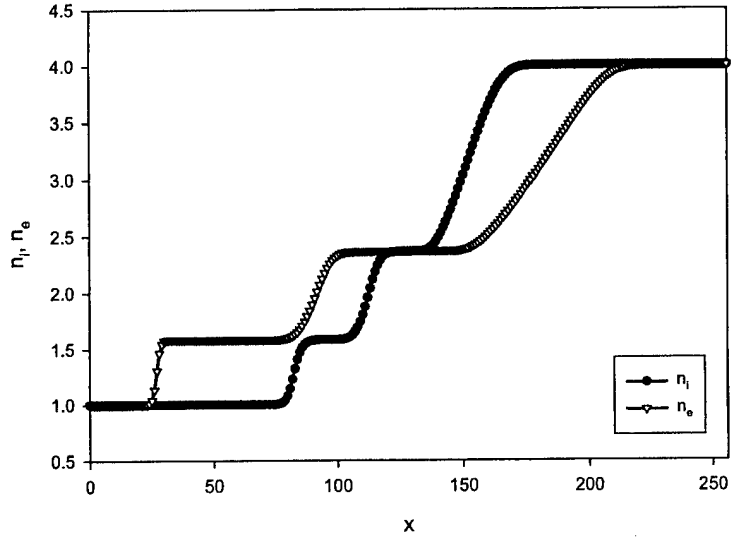
Figure 4: Electron and ion number densities for a shock tube simulation. The shock wave, contact discontinuity, and rarefaction wave can be seen in each fluid.
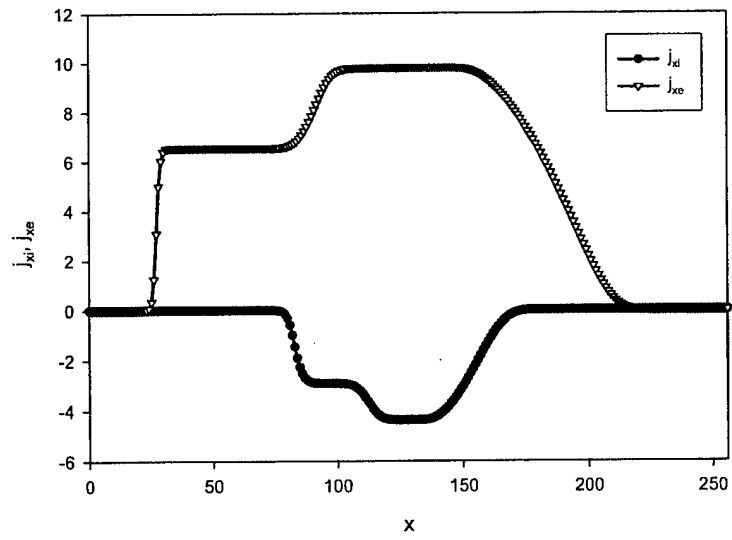

Figure 5: Electron and ion current densities for a shock tube simulation.
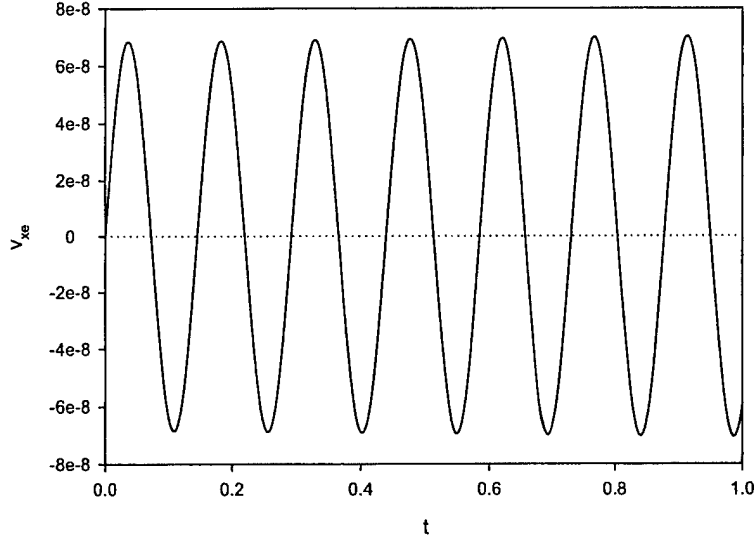
13

Figure 6: Time history of the electron velocity measured at a fixed spatial location demonstrating Langmuir plasma oscillations.

ion number densities after 150 time steps. The characteristic shock wave, contact discontinuity, and rarefaction wave are clearly evident in both the electron and ion fluid. The more massive ion fluid has slower characteristic wave speeds. The sound speed varies like the squareroot of the mass. Fig. 5 shows the evolution of the electron and ion current densities in the longitudinal direction after 150 time steps. When the effect of the electromagnetic fields is included, the faster electron fluid is slowed by the slower, massive ion fluid. The number density jumps are altered as the flow is limited by ambipolar motion.

3.3 Langmuir Oscillations

The ability to capture gas dynamic waves as shown in the coplanar Riemann problem is expected from an approximate Riemann solver. The approximate Riemann solver for two fluid plasma model must also capture plasma wave behavior. This ability is demonstrated by simulating Langmuir plasma oscillations. Langmuir plasma oscillations are the plasmas response to charge concentrations created by perturbations in the plasma. In one dimension, the equation of motion for electrons reduces to a second order differential equation for the particle position.

$$\frac{d^2 x}{dt^2} = -\frac{n_e e^2}{m_e \epsilon_o} x = -\omega_{pe}^2 x \tag{37}$$

where ω_{pe} is the electron plasma frequency. If the plasma pressure is negligible and the fluid velocity is sufficiently small, the two fluid plasma model can produce Langmuir plasma oscillations. A sinusoidal perturbation is initialized to the electron fluid.
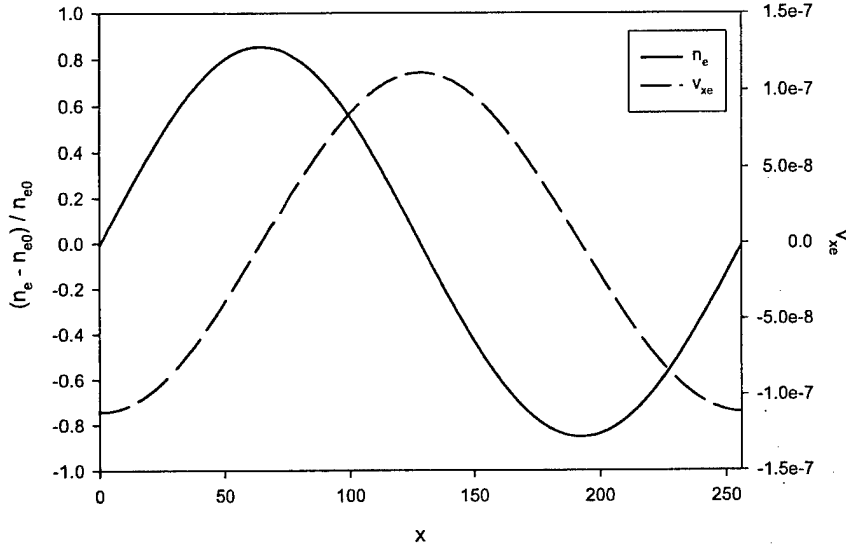
14

Figure 7: Spatial structure of the electron density and velocity at single time during a Langmuir plasma oscillation simulation.

The results are shown in Figs. 6 and 7. The theoretical plasma frequency as determined from the previous equation is $\omega_{pe} = 0.1466$ for the normalized plasma parameters used in the simulation. The numerically generated frequency of $\omega_{pe} = 0.1462$ agrees with the theoretical value with an error of 0.27%.

Though the results presented are from a simplified version of the proposed algorithm, the success and accuracy of the simulations demonstrate the ultimate potential for a new algorithm based on the two-fluid plasma model.

3.4 Debye shielding

In this problem sheet of charge is introduced near the center of the domain to an otherwise neutral plasma. The electrons and ions respond to shield out the electric field. The modified Maxwell's equations are used in this simulation because charge separation is the primary effect for this problem which has $\lambda_D/L = 0.1$, so it is important to maintain the correct divergence of the electric field. Furthermore, when the divergence correction is not used, the electric field at the center of the domain decays and the information about the static charge distribution is lost. This is a dynamic simulation which is stopped when the numerical dissipation brings the solution to a steady state.

For the simulation results presented in Figs. 8 and 9, 1000 grid points are used. Without the sheet of charge the number densities would be uniform. Without the charged fluids the electric field would be uniform. The analytical solution is plotted in Fig. 9 for comparison.

The analytical solution assumes constant temperature with $T_i = T_e$. The number densities are assumed to be perturbed such that $n_i = n_{i0}(1-\delta)$ and $n_e = n_{e0}(1+\delta)$ where $n_{i0} = n_{e0}$. Thermal conductivity is neglected from the calculated two-fluid solution, so
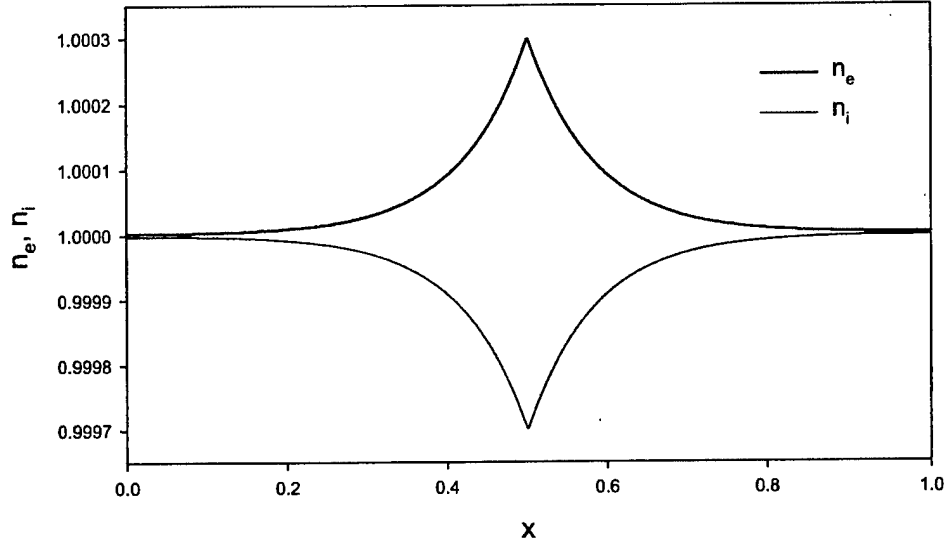
15

Figure 8: Spatial structure of the electron and ion number densities showing the charged fluids response to the sheet of charge.
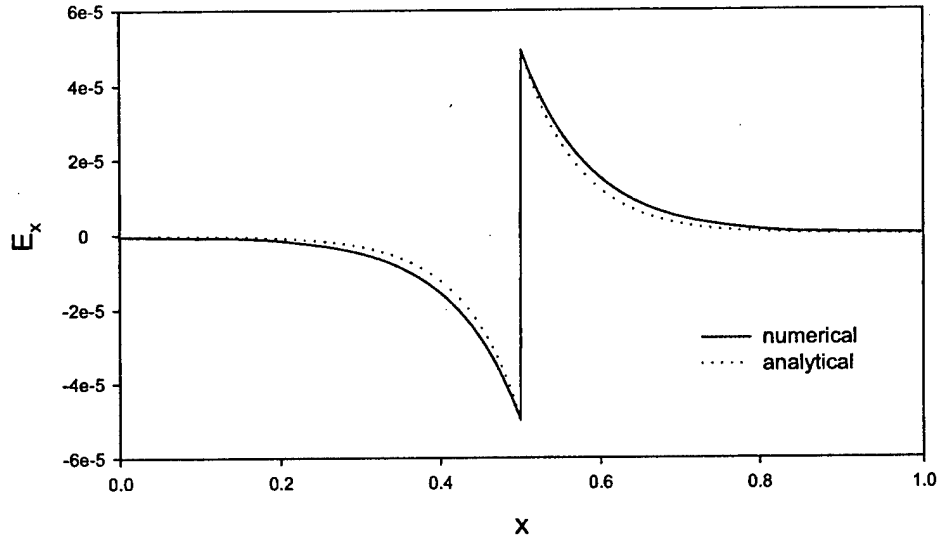

Figure 9: Spatial structure of the electric field showing the shielding effect. Without the charged fluids the electric field would be uniform. The analytical solution for this problem is shown by the dotted line for comparison.
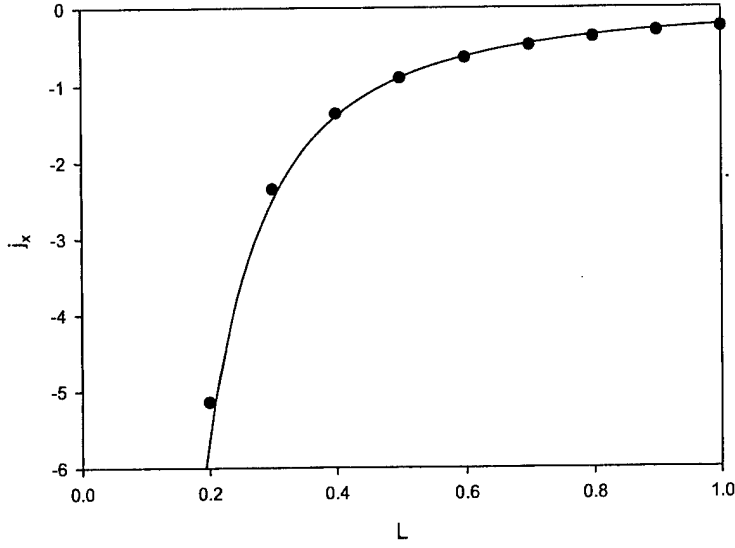
Figure 10: The variation of the Child-Langmuir space charged limited current as the distance between the electrodes are adjusted. The data points are from numerical simulations, and the solid curve is predicted by the theory [eqn(38)].

the steady state solution is not in perfect thermal equilibrium which may explain the discrepancy with the exact solution in Fig. 9.

3.5 Child-Langmuir Current Saturation

The most significant accomplishment during this grant period has been the development of the approximate Riemann solver for the two-fluid plasma model. This section briefly describes the progression of the development.

A fundamental limitation of MHD algorithms is the inability to capture inherently two fluid behavior, such as space charge effects. Space charge effects can occur when finite electric potentials are applied to the plasma or when the plasma comes in contact with insulating or conducting walls. Space charge effects can be investigated by considering an applied electric potential across a vacuum with a plasma fluid at the boundary. The electron plasma fluid (for example) is extracted from the boundary and accelerated through the potential until it leaves the opposite boundary of the domain. Since the plasma is extracted from the boundary with negligible velocity before it is accelerated, the electron fluid density increases and a space charge, virtual cathode tends to form at the boundary. The virtual cathode retards the extraction of additional plasma from the boundary. The space charge effect limits the extracted current according to the Child-Langmuir law.

$$j_{CL} = \frac{4\epsilon_o}{9L^2} \sqrt{\frac{2e}{m_e}} \phi^{3/2} \tag{38}$$

17

which determines the saturation current obtained for an electrode spacing of L and an applied potential of ϕ.

Child-Langmuir current saturation is simulated with the two fluid algorithm. The results are presented in Fig. 10. The data presented illustrate the variation of the saturation current as the spacing between the electrodes is adjusted. The data points are generated from the numerical simulations, and the solid curve is the plot of eqn(38). The error in the fit at the extreme values of the potential are the result of numerical dissipation of the first-order flux calculation. It is expected that the fit would improve with a higher-order method.

4 Professional Interactions

4.1 Project Personnel

The personnel who have been directly involved in this project are listed below.

Name	Position
Uri Shumlak	Assistant Professor
D. Scott Eberhardt	Associate Professor
Thomas R. Jarboe	Professor
Chris Aberle	Graduate Student
John Loverich	Graduate Student

4.2 Collaborations

4.2.1 Air Force Research Laboratory

Dr. Robert Peterkin, Jr. of the Electromagnetic Sources Division of the Air Force Research Laboratory at Kirtland AFB on three-dimensional multigrid algorithms for MACH3 an development of a parallel PIC (particle in cell) code for microwave simulations. Knowledge developed in the area of relaxation schemes was implemented into the ICEPIC code to make a 3-D Poisson solver. The solver was needed to determine electric field concentration on a high power microwave source.

4.2.2 University of Washington

Prof. Scott Eberhardt of the Aeronautics and Astronautics Department and Prof. Randy LeVeque of the Applied Math Department on approximate Riemann solvers and their applications to multidimensional problems, in particular, the correction to transverse fluxes.

Prof. Tom Jarboe of the Aeronautics and Astronautics Department on the MHD stability simulations of spheromaks in realistic three-dimensional geometries and the beta pressure limit of driven spheromak plasmas. This is an ongoing collaboration that resulted in several publications and an experimental project for Prof. Jarboe.

4.3 Publications

Two papers describing this project and related research were presented at the AIAA Computational Fluid Dynamics conference. One paper titled "An Approximate Riemann Solver for MHD Computations on Parallel Architectures" provided an overview

18

of the project. The other paper titled "Application of Analytical Methods to Computing Numerical Flux Jacobians" described the work on the analytical flux Jacobian calculation.

5   Conclusions

The research accomplishments of this research effort represent significant advances in the field of plasma dynamic simulations. This advancement is important because plasma researchers are increasingly finding that the assumptions made in the single-fluid MHD model are too restrictive to model selected plasma dynamic phenomena, and currently two-fluid plasma simulation codes have been limited to linearized models with only two spatial dimensions. The accomplishments indicate that the proposed research goals are being met.

The successful development of a one-dimensional algorithm based on the two-fluid plasma model demonstrates the potential of the project, and it indicates that this project is reaching its objectives. The research related to this project has been presented at international conferences. Valuable collaborations have been formed with the Air Force Research Laboratory.

The continuing development of this project will include making the algorithm more robust to handle electromagnetic fields, develop an electromagnetic solver for arbitrary, cell-centered grids, and extending the algorithm to three-dimensions.

References

[1] A. R. Bell, Astrophys. Space Sci. **256**, 13 (1998).

[2] C. Z. Cheng and G. Knorr, J. Comput. Phys. **22**, 330 (1976).

[3] H. Ruhl and P. Mulser, Phys. Lett. **A205**, 388 (1995).

[4] L. Chacón, D. C. Barnes, D. A. Knoll, G. H. Miley, J. Comput. Phys. **157**, 618 (2000).

[5] L. Chacón, D. C. Barnes, D. A. Knoll, G. H. Miley, J. Comput. Phys. **157**, 654 (2000).

[6] C. K. Birdsall and A. B. Langdon, *Plasma Physics via Computer Simulation*, McGraw-Hill, New York (1985).

[7] J. P. Freidberg, Rev. Mod. Phys. **54**, 801 (1982).

[8] R. E. Peterkin, Jr., M. H. Frese, and C. R. Sovinec, J. Comput. Phys. **140**, 148 (1998).

[9] U. Shumlak, T. W. Hussey, and R. E. Peterkin, Jr., IEEE Trans. Plasma Sci. **23**, 83 (1995).

[10] O. S. Jones, U. Shumlak, D. S. Eberhardt, J. Comput. Phys. **130**, 231 (1997).

[11] B. Udrea and U. Shumlak, "Non-linear Study of the Spheromak Tilt Instability," AIAA-98-0995 (1998).

[12] U. Shumlak and B. Udrea, "An Approximate Riemann Solver for General Finite Volumes," to be submitted to J. Comput. Phys.

19

[13] O. S. Jones, "Study of Magnetic Relaxation in Plasmas Using a Parallel Implicit MHD Solver," Ph. D. Dissertation, University of Washington (1997).

[14] B. Udrea, "An Advanced Implicit Solver for MHD," Ph. D. Dissertation, University of Washington (1999).

[15] U. Shumlak, "Development of an Advanced Implicit Algorithm for MHD Computations on Parallel Supercomputers," Final Technical Report to AFOSR, Feb. 1999.

[16] U. Shumlak, "An Implicit, Conservative Multi-Temperature MHD Algorithm," Final Technical Report to AFOSR, Feb. 2000.

[17] D. Harned and Z. Mikic, J. Comput. Phys. **83**, 1 (1989).

[18] J. T. Becerra Sagredo, "Semi-implicit Treatment of the Hall Term in Finite Volume, MHD Computations," M. S. Thesis, University of Washington (1998).

[19] N. A. Krall and A. W. Trivelpiece, *Principles of Plasma Physics,* McGraw-Hill, New York (1973).

[20] P. L. Roe, J. Comput. Phys. **43**, 357 (1981).

[21] C. D. Munz, R. Schneider, and U. Vos, SIAM J. Scientific Computing **22**, 449 (2000).

[22] P. L. Roe, J. Comput. Phys. **135**, 250 (1997).